MINIATURIZED GPS ANTENNA ARRAY TECHNOLOGY

Alison Brown, Dale Reynolds, Huan-Wan Tseng; *NAVSYS Corporation*.
John Norgard, *University of Colorado at Colorado Springs*

ABSTRACT

NAVSYS have developed a miniaturized GPS antenna array technology that reduced the size of the antenna elements and the array dimensions. This technology enables GPS controlled radiation pattern antenna arrays (CPRAs) with anti-jamming capability to be installed on vehicles where their size has previously prohibited their use. This includes small munitions, such as Joint Direct Attack Munition (JDAM), and aircraft where size and weight constraints resulted in fixed pattern radiation antenna (FRPA) installations. The miniaturized GPS antenna array uses high dielectric material to reduce the size of the antenna elements and reduce the separation between the elements. This design approach allows the size of the antenna array to be significantly reduced. NAVSYS have built and tested a four element miniaturized array that can fit in a six-inch footprint. In this paper, the miniaturized antenna array technology is described and test results are included showing the antenna array characteristics. This includes input impedance, voltage standing wave ratio (VSWR), reflection coefficient, and mutual coupling data, antenna pattern and standard antenna element comparison data from anechoic chamber measurement, and also antenna array gain and array element phase relationship taken with the miniaturized antenna integrated with GPS digital beamforming electronics.

GPS ANTI-JAM ANTENNA ARRAYS

The low broadcast power of the GPS satellites (approximately -160 dBw) makes these signals particularly susceptible to jamming. Figure 1 shows the jammer/signal (J/S) power levels as a function of distance and jammer transmit power (assumes a line of sight path and a received P(Y) code power of -163 dBw). The current generation of GPS User Equipment (UE) relies on using the more susceptible C/A code for signal acquisition. As shown in Figure 1, this can be denied almost to the horizon with as little as 22 dB J/S. If precise time is known, then P(Y) code signal acquisition can occur directly and will not be denied until the J/S exceeds 34 dB. With advanced signal processing techniques, GPS acquisition can be achieved under J/S as high as 44 dB. However, as shown in Figure 1, even a relatively low power jammer can have drastic effect on GPS receivers at quite significant distances from the jammer source.

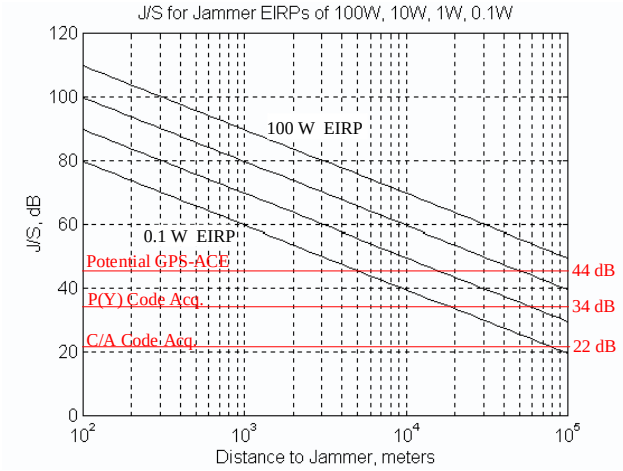

Figure 1 Jammer effects versus distance

The most effective performance improvements against jammers are provided through the use of controlled radiation pattern antennas (CRPAs). These antennas increase the J/S margin to 84 dB with a conventional GPS receiver and further improvements to 98 dB can be expected with advanced receiver designs.

The basic design of a simple beam-steering or null-forming antenna array is illustrated in Figure 2. The simple example shown consists of four microstrip patch antenna elements with antenna weighting and phase

shifter circuitry to adapt the array pattern. More advanced anti-jam (A/J) electronics are currently under development by the USAF using adaptive digital signal processing algorithms. The miniaturized antenna design is being developed to be compatible with the A/J electronics currently in use with conventional CRPA arrays [1] or the newer GPS Antenna System (GAS). All these A/J systems are designed to detect multiple jammer signals and place a null in the antenna pattern in the location of the jammer.

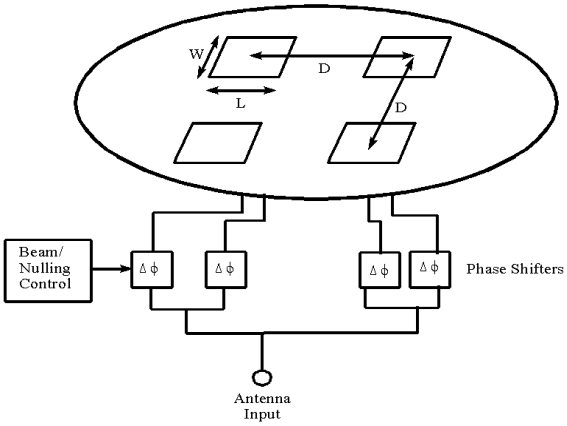

Figure 2 Basic phased array antenna design

GPS MINI-ARRAY CONCEPT

A key factor in the array performance is the number of antenna elements. The more elements available, the more precisely a null can be steered in the direction of a jammer, improving the overall SNR and also allowing flexibility in placing nulls on jammers. The number of jammers which can be nulled by a GPS array is equal to one less than the number of antenna elements (N-1). The more elements in a beam forming array, the greater the degree of directionality in the array and the greater the gain in the direction of the desired signals.

To prevent spatial correlation, the antenna array elements in a conventional array must be placed half a wavelength apart. This changes the relative phase shift between elements as a function of the input signal elevation angle so that there is no phase shift (0^o) when the signal is perpendicular to the array and a half cycle phase shift between elements (180^o) when the signal is horizontal to the array.

As described in this paper, it is possible to shrink the size of the individual antenna elements by designing small patch elements using a high dielectric substrate. This will allow more antenna elements to be clustered closer together in the same over-all array footprint. The major innovation presented in this research effort is the introduction of a shaped high-dielectric superstrate, which allows reduction in the mutual coupling between elements and the same half-cycle phase relationship to be maintained between antenna elements as in a full-size array. The combination of these effects enable the over-all size of a GPS antenna array to be shrunk while still providing equivalent A/J protection to a full-size conventional GPS CRPA. This will allow the existing 7-element CRPA array of 14-inch diameter to be reduced to less than 6 inches in diameter.

GPS MINI-ARRAY APPLICATIONS

Many of the smaller munitions in operation or in development do not have a form factor that allows for a conventional CRPA to be installed. Because of size and weight constraints, some host aircraft within the Air Force and Navy have also elected to install FRPA antennas which cannot provide the A/J protection needed in many tactical environments. The GPS mini-array will enable A/J capability to be provided on many small munitions, aircraft and other host vehicles where the size and weight of the conventional CRPA array has previously been prohibitive. For example, current programs, such as the Joint Direct Attack Munition (JDAM), Joint Air-to-Surface Standoff Missile (JASSM), and the Joint Standoff Weapon (JSOW), will be able to benefit from the reduced size but full performance of the mini-array technology.

MINI-ARRAY DESIGN OVERVIEW

The miniature array is composed of a ground plane, a substrate with the antenna elements on its surface, and a superstrate on top of the elements. The dielectric constant of the substrate is increased so that the size of the antenna elements can be reduced. This allows the antenna element spacing to be reduced. By controlling the design of the antenna elements, the efficiency is increased so that they have the same gain as a standard GPS antenna element. By adjusting the dielectric constant and shape of the superstrate, the mutual coupling between the antenna elements is minimized and the reduced antenna spacing is scaled so that it appears to be effectively $\lambda/2$ in its beamforming or null steering performance.

A summary of the mini-array specifications is shown below in Table 1. As can be seen, the array was designed for receiving the GPS L1 frequency with sufficient bandwidth to receive both C/A code and P code versions of GPS data. To provide optimum performance as a CRPA, its elements have been arranged into a square with $\lambda/2$ antenna spacing. Figure 3 displays the top view of the current mini-array configuration.

Table 1 Summary of mini-array specification

Center Frequency	1575.42 MHz (at L1)
Bandwidth	20 MHz (1575.42 +/- 10 MHz)
Input Impedance	50 Ohms
Polarization	Right Hand Circular Polarization (RHCP)
Array Size	6 Inches Diameter
Array Configuration	Square
Number of Elements	4
Element Type	Rectangular
Feed Arrangement	Probe Feed

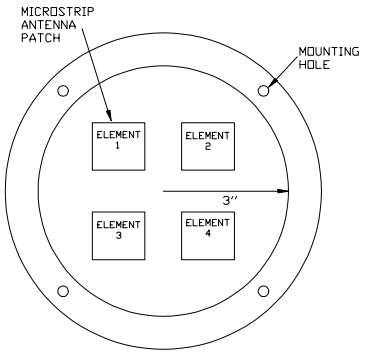

Figure 3 Top view of the 4-element mini-array configuration

MINI-ARRAY DESIGN TOOLS

The Method of Moments (MOM) model shown in Figure 4 was selected to aid in the design of the antenna elements. Since the antenna element patch size and feed point placement is a function of both the substrate and the superstrate, a computer model is needed in helping select the optimum parameters to maximize the miniature array overall performance.

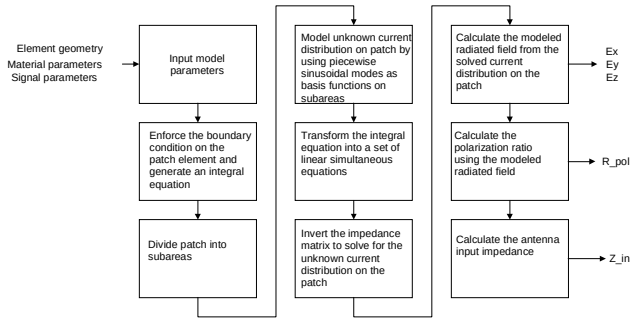

Figure 4 Method of Moments (MOM) flow diagram for antenna element design

MEASUREMENT RESULTS

Input Impedance

The input impedance of each of the four elements is close to 50 ohms at the L1 frequency. A typical measured input impedance versus frequency is shown in Figure 5.

Voltage Standing Wave Ratio (VSWR)

The measured VSWR for each of the four elements is less than 2.0:1 within a frequency band of 1575.42 +/- 10.0 MHz. A typical measured VSWR versus frequency is shown in Figure 6.

Reflection Coefficient

The measured reflection coefficient of the mini-array antenna elements is close to 0 within the L1 frequency band. A typical measured reflection coefficient is shown in Figure 7.

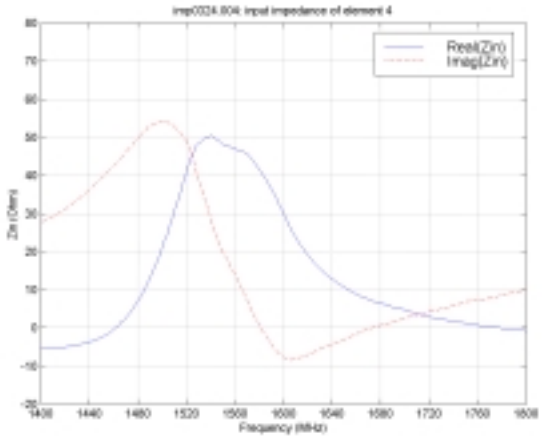

Figure 5 The measured input impedance of one element of the mini-array

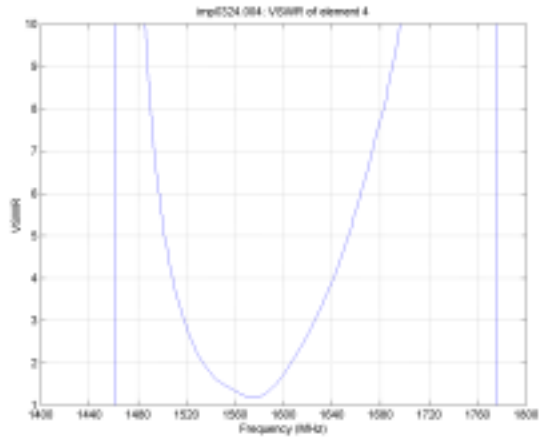

Figure 6 The measured VSWR of one element of the mini-array

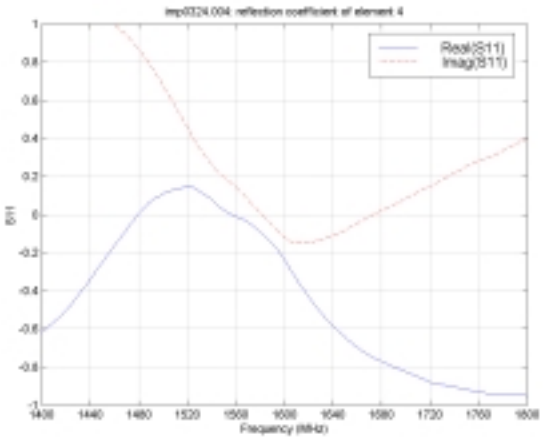

Figure 7 The measured reflection coefficient of one element of the mini-array

Mutual Coupling

The transmission coefficient between the elements is used to indicate the mutual coupling between them. The strongest mutual coupling occurs between Element 2 and Element 3, and the transmission coefficient is below –14 dB in the L1 frequency band (1575.42 +/- 10 MHz). Figure 8 and Figure 9 show two typical measured transmission coefficients between the four elements of the mini-array.

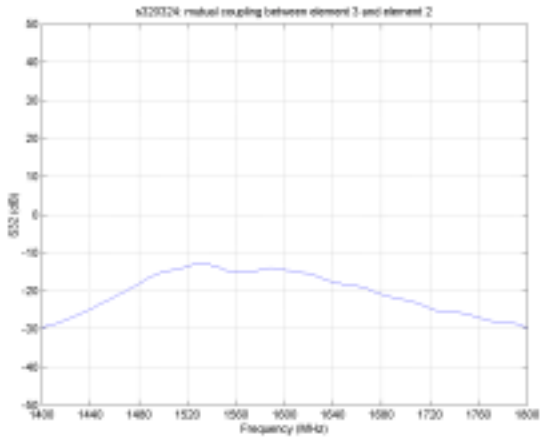

Figure 8 The measured transmission coefficient between element 3 and element 2

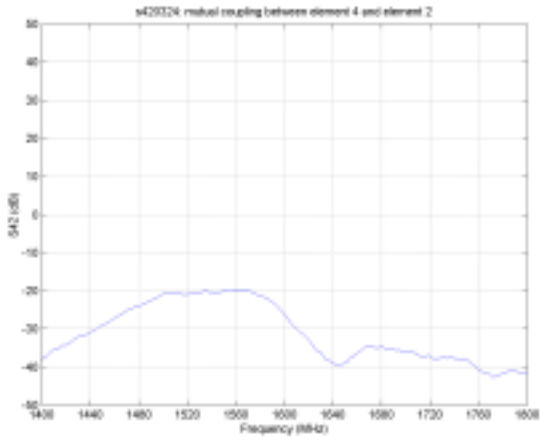

Figure 9 The measured transmission coefficient between element 4 and element 2

Antenna Receiving Pattern

The antenna receiving patterns of the mini-array antenna element were measured inside the Microwave Anechoic Chamber (MAC) at the Electromagnetic Laboratory (EML) of the University of Colorado at Colorado Springs (UCCS). Both x-z plane and y-z plane (where z axis is perpendicular to the surface of the antenna patch) receiving patterns with both E_ϕ and E_θ incident waves were measured. There was a 3-foot square flat metal ground plane behind the mini-array antenna element during measurements. Figure 10 and Figure 11 show the typical measured antenna receiving patterns. As shown in these figures, the mini-array antenna element has a broad receiving pattern as can be expected from a small patch element.

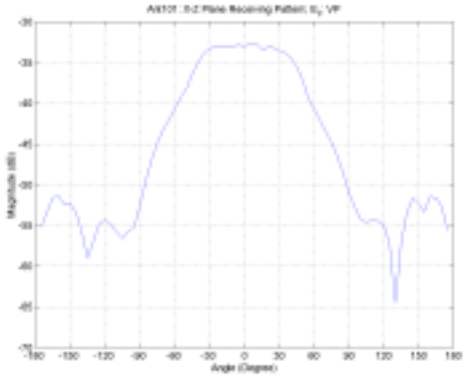

Figure 10 The x-z plane receiving pattern with E_ϕ incident waves for the mini-array antenna element

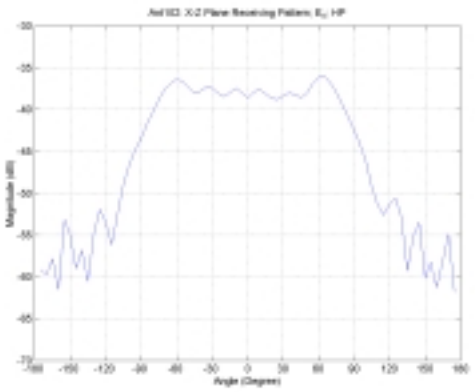

Figure 11 The x-z plane receiving pattern with E_θ incident waves for the mini-array antenna element

Received Power Level Comparison

A commercially available GPS antenna from AeroAntenna Technology (Model AT575-97B-SMAF-000-00-00-NM) was used as the reference antenna for receive power level comparison. According to the data sheet, this reference antenna has the following radiation coverage:

4.0 dBic	$\theta = 0^\circ$
-1.0 dBic	$0^\circ < \theta < 75^\circ$
-2.5 dBic	$75^\circ \le \theta < 80^\circ$
-4.5 dBic	$80^\circ \le \theta < 85^\circ$
-7.5 dBic	$\theta = 90^\circ$

The test facility, the test equipment, the test set-up, and the test procedures for the reference antenna were exactly the same as those for the mini-array antenna element. Figure 12 and Figure 13 show the typical measured antenna receiving patterns of this reference antenna. In the main beam directions, the receive power level of this reference antenna stays nearly constant at –35 dB. Our mini-array antenna element has two receive power levels, one at –32.5 dB and the other at –38.5 dB, depending on the polarization of the incident waves and the plane of measurements. In terms of the polarization ratio, the reference antenna is circularly polarized, and our mini-array antenna element is elliptically polarized. Although there is still room for improvement in this regard, our mini-array antenna element can support the RHCP operation.

Antenna Array Gain Measured with the NAVSYS High Gain Advanced GPS Receiver (HAGR)

The NAVSYS HAGR is a GPS digital beamforming electronic system which consists of a digital front end (DFE) unit, a digital beam-steering (DBS) card, a correlation accelerator chip (CAC) board, and the associated software [2]. The DFE unit converts the L1-band radio frequency (RF) signals to digital signals. The HAGR-DFE unit can be configured to include up to 16 DFE channels, each connecting to one antenna element. The digital data from the DFE outputs are processed by the DBS card to provide a composite signal output for each satellite being tracked. There are 8 DBS channels, and each can be used to provide the composite signal for a single satellite. The CAC board contains the correlator chips that perform the code correlations and the complex multiplications needed for code and carrier tracking of GPS satellite signals. There are 8 CAC channels each connecting to a single DBS channel.

The test set-up was approximately 40 feet away from the NAVSYS building, and a 3'x3' metal plate was used as the ground plane for the 4-element mini-array. The mini-array enables the HAGR to continuously track the satellites and update the navigation data. Figure 14 to Figure 19 display the measured C/N0 values from satellite PRNs 30, 24, 10, 5, 4, and 8 for the 4-element mini-array with a NAVSYS HAGR and a single AT575-97 reference antenna with a Novatel GPS receiver. On average, the 4-element mini-array provides a gain of 4 to 5 dB in C/N0 as compared to the AT575-97 reference antenna.

Figure 12 The x-z plane receiving pattern with E_ϕ incident waves for AeroAntenna Technology's AT575-97B-SMAF-000-00-00-NM GPS antenna

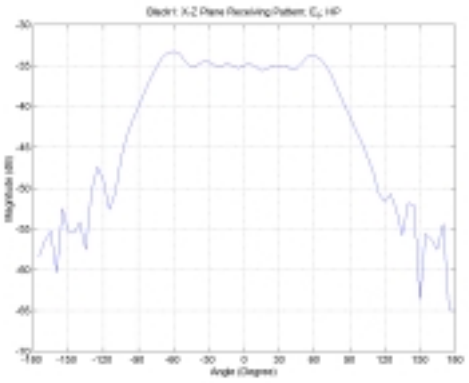

Figure 13 The x-z plane receiving pattern with E_θ incident waves for AeroAntenna Technology's AT575-97B-SMAF-000-00-00-NM GPS antenna

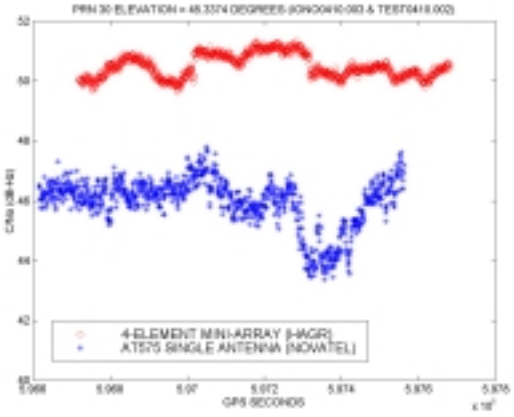

Figure 14 The measured C/N0 values from PRN 30 for the 4-element mini-array with a NAVSYS HAGR and for an AT575-97 reference antenna with a Novatel receiver

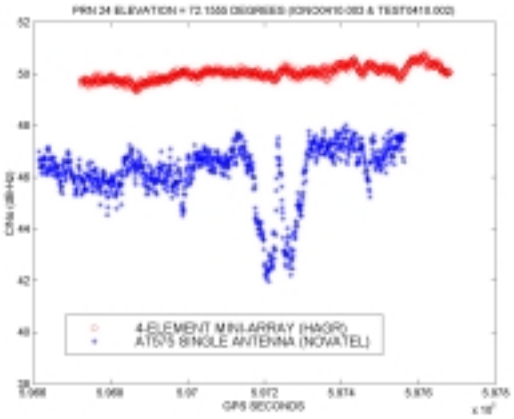

Figure 15 The measured C/N0 values from PRN 24

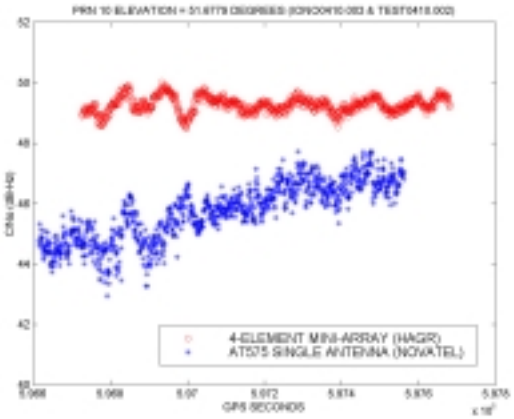

Figure 16 The measured C/N0 values from PRN 10

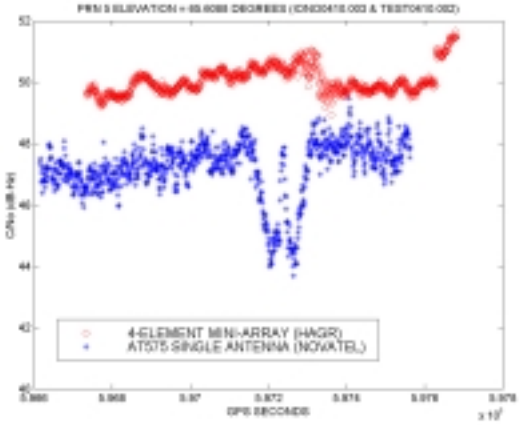

Figure 17 The measured C/N0 values from PRN 5

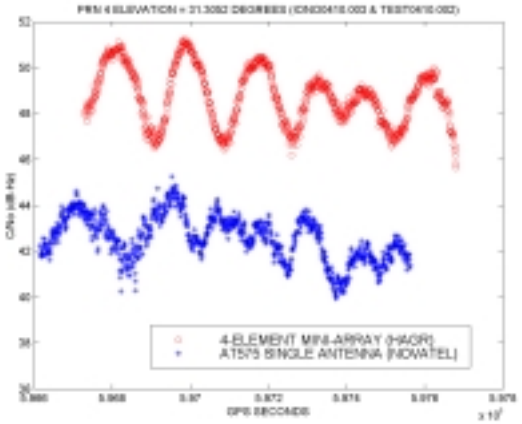

Figure 18 The measured C/N0 values from PRN 4

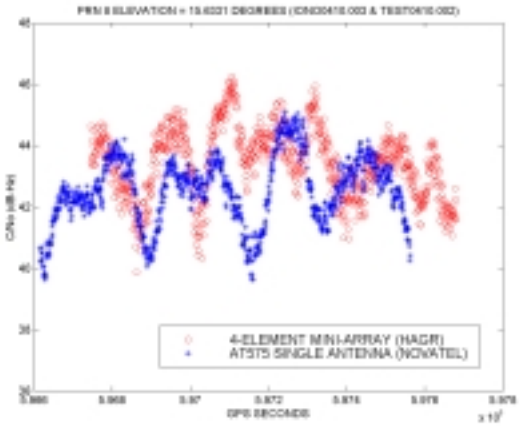

Figure 19 The measured C/N0 values from PRN 8

Measured GPS Carrier Signal's Phase Difference between Mini-Array Antenna Elements

Figure 20, Figure 21, and Figure 22 show the HAGR satellite measurement of the GPS carrier signal's phase difference between Elements 2, 3, 4 and Element 1 (reference element) of the 4-element mini-array. The incident angle in these figures is the arc cosine of the inner product of the base-line unit vector and the line-of-sight unit vector, where the azimuth and elevation angles are from the satellites. Figure 20 and Figure 21 show that the effective spacing between elements 2-1 and elements 3-1 is close to 0.5 cycle, and Figure 22 shows that the effective spacing between elements 4-1 (in diagonal positions of the square array configuration) is close to 0.707 cycle. The spread of the measured data in these three figures is due to the multipath effect. In order to remove this multipath phenomenon, the experiment should be conducted in a controlled environment such as an electromagnetic anechoic chamber.

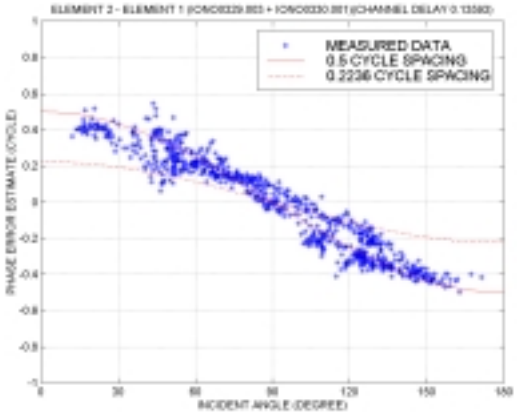

Figure 20 The HAGR satellite measurement of the GPS carrier signal's phase difference between Element 2 and Element 1 of the 4-element mini-array

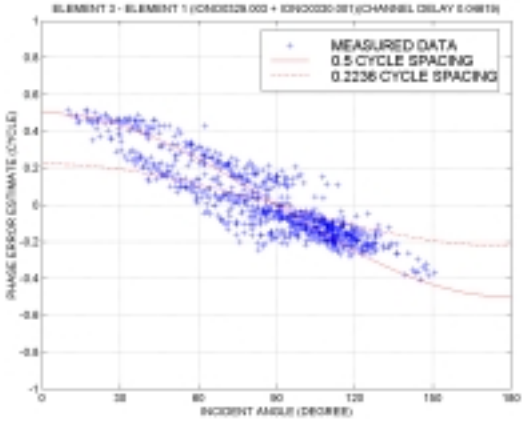

Figure 21 The HAGR satellite measurement of the GPS carrier signal's phase difference between Element 3 and Element 1 of the 4-element mini-array

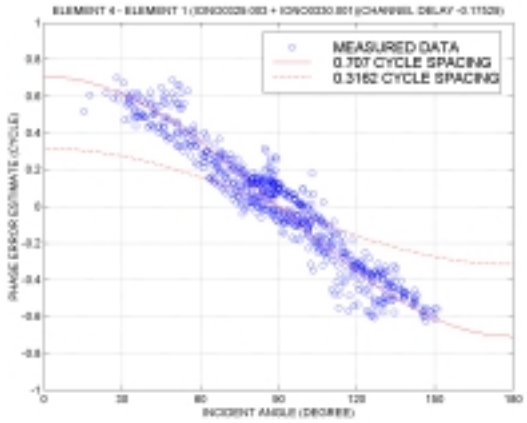

Figure 22 The HAGR satellite measurement of the GPS carrier signal's phase difference between Element 4 and Element 1 of the 4-element mini-array

Anechoic Chamber Measurements of the GPS Carrier Signal's Phase Difference between Mini-Array Antenna Elements

Figure 23, Figure 24, and Figure 25 show the measured phase difference between elements 1-3, 4-3, and 2-3 versus the elevation angle in the y-z plane for E_θ incident waves. As shown in these figures, the phase difference between elements 1-3 and 2-3 is very close to 0.5 cycle when the elevation angle is 0 degrees. Also, the phase difference between elements 4-3 is very close to 0 cycle as expected since the base-line vector is perpendicular to the line-of-sight vector. It is noted that the actual physical spacing between adjacent elements is only 0.2236 cycle in free-space.

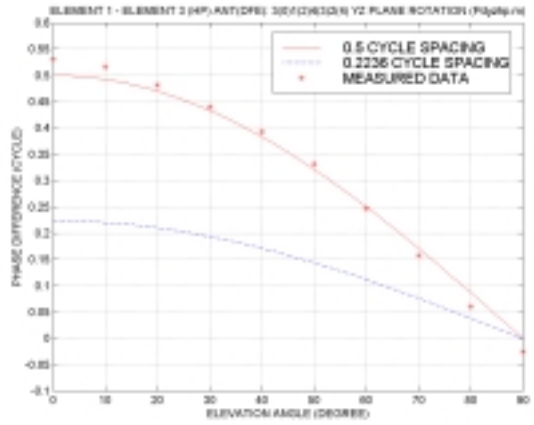

Figure 23 The measured phase difference between Element 1 and Element 3 (reference element) versus elevation angle in the y-z plane for E_θ incident waves

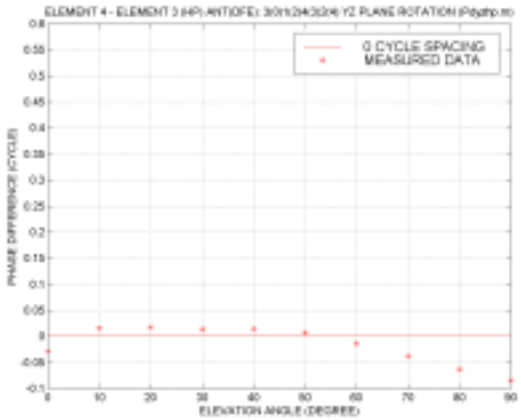

Figure 24 The measured phase difference between Element 4 and Element 3 (reference element) versus elevation angle in the y-z plane for E_θ incident waves

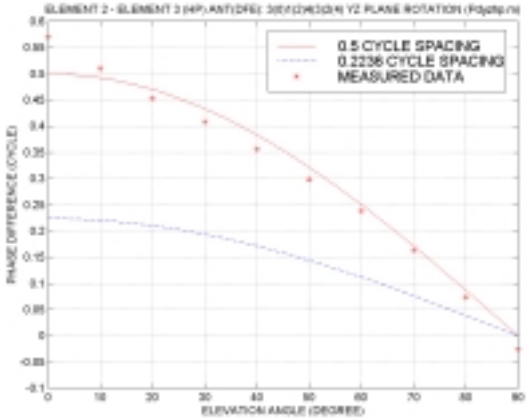

Figure 25 The measured phase difference between Element 2 and Element 3 (reference element) versus elevation angle in the y-z plane for E_θ incident waves

CONCLUSION

The purpose of this research effort was to design and fabricate a miniaturized antenna array for GPS applications that can be used to provide GPS anti-jamming enhancements. The following technical objectives have been achieved.

Design, build and test prototype patch antenna elements with high dielectric substrate and high dielectric superstrate

A method of moments design tool was built to design patch elements for use in the miniature antenna array. The antenna element, designed to be compatible with the mini-array high dielectric superstrate and substrate material, gave similar performance to a conventional GPS antenna used as a reference.

Analyze boundary effects between the superstrate and free space

A design tool was developed to analyze the phase shifts predicted between the antenna elements in a mini-array caused by the superstrate. This design tool was used to analyze the predicted phase difference and A/J performance of the miniaturized antenna array.

Test each array pattern for a variety of progressive phase arrangements for comparison with simulated patterns

The 6" form factor mini-array was tested in an anechoic chamber and with live satellite observations to compare the measured phase relationship between elements with the phase relationship predicted using the mini-array simulation tools. The simulation tools predicted that the miniature antenna array phase relationship should be within 0.05 cycles of a full size antenna array. The anechoic chamber observations showed excellent agreement with these results.

Measure the performance of the miniaturized array by demonstrating satellite tracking with an L1 GPS receiver

The phase angle between the antenna elements was also observed using live GPS satellite tracking. These results are shown in Figure 20 to Figure 22. The noise on the phase observations is caused by carrier multipath between the antenna elements. This is typically on the order of +/- 0.1 cycles. However, the plots clearly show that the mean carrier phase offset between the antenna elements follows the predicted half-wavelength phase variation demonstrating that the high dielectric lens is having the predicted effect on the GPS signals. The NAVSYS digital beam steering High Gain Advanced GPS Receiever (HAGR) was used to demonstrate the antenna array performance. By applying the predicted ½ wavelength phase shifts to each antenna element digitally, the HAGR forms a phase coherent signal sum from each of the 4 antenna elements which is predicted to have a theoretical 6 dB gain improvement over a single element GPS receiver. In Figure 14 to Figure 19, the C/N_0 from the GPS satellites tracked are shown compared with a conventional GPS receiver. These show that the mini-array is providing 4 to 5 dB gain per satellite as expected.

In conclusion, this research effort has successfully demonstrated a technique for miniaturizing a GPS phase array antenna. We achieved our objective of developing and testing a 4-element antenna array in a 6" form factor and demonstrating that its performance is equivalent to a full-size array with ½ wavelength separation.

ACKNOWLEDGEMENT

This work was sponsored under the Office of Naval Research SBIR contract N00014-98-C-0042, "Miniaturized GPS Antenna Arrays Using High Dielectric Materials."

REFERENCES

[1] Critical Item Development Specification for the Controlled Reception Pattern Antenna (CRPA) Line Replaceable Unit (LRU) of the NAVSTAR Global Positioning System Antenna System-1 (GAS-1), CI-GAS1/CRPA-300A, Appendix II to SS-GAS1-300A, 24 Apr 1998.

[2] 'Test Results of a High Gain Advanced GPS Receiver,' Alison Brown and Gengsheng Zhang, ION 55th Annual Meeting.